

PHASE TRANSITIONS IN TETRAHEDRAL ISING LATTICES

A THESIS

SUBMITTED TO THE DEPARTMENT OF PHYSICS
AND THE INSTITUTE OF ENGINEERING AND SCIENCES
OF BILKENT UNIVERSITY
IN PARTIAL FULFILLMENT OF THE REQUIREMENTS
FOR THE DEGREE OF
MASTER OF SCIENCE

By

Alkan Kabakçıoğlu

May 12, 1993

QC
175.16
.P5
K33
1993

PHASE TRANSITIONS IN TETRAHEDRAL ISING
LATTICES

A THESIS

SUBMITTED TO THE DEPARTMENT OF PHYSICS
AND THE INSTITUTE OF ENGINEERING AND SCIENCES
OF BILKENT UNIVERSITY
IN PARTIAL FULFILLMENT OF THE REQUIREMENTS
FOR THE DEGREE OF
MASTER OF SCIENCE

Alkan Kabakçiođlu
tarafından hazırlanmıştır.

By

Alkan Kabakçiođlu

May 12, 1993

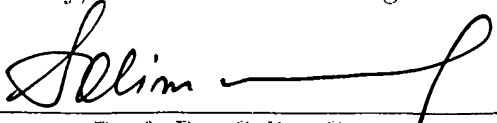
JC
175.16
.P5
K33
1993

B000957

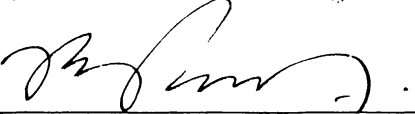
I certify that I have read this thesis and that in my opinion it is fully adequate, in scope and in quality, as a thesis for the degree of Master of Science.


Prof. Dr. Cemal Yalabık(Principal Advisor)


I certify that I have read this thesis and that in my opinion it is fully adequate, in scope and in quality, as a thesis for the degree of Master of Science.


Prof. Dr. Salim Çıracı

I certify that I have read this thesis and that in my opinion it is fully adequate, in scope and in quality, as a thesis for the degree of Master of Science.


Assoc. Prof. Dr. Bilal Tanatar

Approved for the Institute of Engineering and Sciences:


Prof. Dr. Melmet Baray
Director of Institute of Engineering and Sciences

ABSTRACT

PHASE TRANSITIONS IN TETRAHEDRAL ISING LATTICES

Alkan Kabakçioğlu

M.S. in Physics

Supervisor: Prof. Dr. Cemal Yalabık

May 12, 1993

After a review of the Renormalization Group theory, the phase diagram of unisotropic tetrahedral Ising lattice is explored by the motivation gained through the recent experimental findings about SiGe alloys. Renormalization Group approach and the mean-field RG approximation previously proposed by Kuzel are used. Four different ordered phases are observed. The critical exponent ν is calculated using the linearized transformation around the fixed points and compared with previous works. It is concluded that the newly observed orderings in SiGe superlattices are induced by surface effects.

Keywords: Phase transition, critical phenomena, Renormalization Group, Ising model, SiGe superlattice.

ÖZET

TETRAHEDRAL ISING ÖRGÜSÜNDE FAZ GEÇİŞLERİ

Alkan Kabakçiođlu
Fizik Bölümü Yüksek Lisans
Tez Yöneticisi: Prof. Dr. Cemal Yalabık
12 Mayıs 1993

Renormalizasyon Grubu teorisinin ele alınmasından sonra, SiGe üstünörgülerine ilişkin yakın zamandaki deneysel bulgulardan esinlenerek eşyönlü olmayan tetrahedral Ising örgüsünün faz şeması incelendi. Yöntem olarak Renormalizasyon Grubu yaklaşımı ve daha önce Kinzel tarafından önerilen RG ortalama-alan yaklaşıklığı kullanıldı. Dört farklı düzenli faz gözlemlendi. Dönüşümün sabit nokta yakınında doğrusallaştırılmasıyla kritik üstel değerlerden ν hesaplandı ve başka çalışmaların bulgularıyla karşılaştırıldı. SiGe üstünörgülerinde yeni gözlenen düzenlenmelerin yüzey etkilerinden kaynaklandığı sonucuna varıldı.

Anahtar kelimeler : Faz geçişi, kritik olaylar, Renormalizasyon grubu, Ising modeli, SiGe üstünörgüsü.

ACKNOWLEDGMENT

I am grateful to Prof. Dr. Cemal Yalabık whose supervision, guidance, valuable suggestions and encouragement made possible the completion of this thesis. His academic personality, understanding and patience are unforgettable.

Special thanks to all members of the Department of Physics for their generous helps and friendship, especially to Erkan, Oguz and Zafer who were ready for help in all cases of emergency.

And very special thanks to my dear family and to Tuba for their moral support which I benefited a lot.

Contents

| | | |
|----------|--|-----------|
| 1 | INTRODUCTION | 1 |
| 2 | PHASE TRANSITIONS AND CRITICAL PHENOMENA | 3 |
| 2.1 | A Review of History | 6 |
| 2.1.1 | Landau Mean Field Theory | 7 |
| 2.1.2 | Experiment Conflicts Theory | 8 |
| 2.2 | Universality and Scaling Laws : The Modern Era | 8 |
| 2.2.1 | Law of Corresponding States | 8 |
| 2.2.2 | Critical Exponents and Scaling Laws | 10 |
| 3 | RENORMALIZATION GROUP | 12 |
| 3.1 | Momentum-Space Renormalization | 13 |
| 3.2 | Position-space Renormalization | 15 |
| 3.2.1 | Spin-decimation method | 15 |
| 3.2.2 | Kadanoff's Block-Spin Method | 17 |
| 3.2.3 | Scaling Hypothesis and Critical Exponent Relations . . . | 18 |
| 3.3 | Linearized RG transformation | 20 |
| 3.3.1 | Calculating ' ν ' | 21 |
| 3.3.2 | Fixed points and critical surfaces | 22 |

| | | |
|----------|---|-----------|
| 4 | PHASE TRANSITIONS IN TETRAHEDRAL ISING LATTICE | 24 |
| 4.1 | Order-disorder transition in SiGe alloys | 24 |
| 4.2 | The model and the RG transformation | 25 |
| 4.2.1 | The model Hamiltonian | 25 |
| 4.2.2 | RG transformation | 28 |
| 4.3 | Results and the Phase Diagram | 30 |
| 4.3.1 | The Phase Diagram | 32 |
| 5 | CONCLUSION | 37 |

List of Figures

| | | |
|-----|--|----|
| 2.1 | Behavior of the free energy of the system in (a) <i>2nd</i> and (b) <i>1st</i> order phase transitions | 5 |
| 2.2 | Phase diagram of water. | 6 |
| 2.3 | Phase diagram for an Ising ferromagnet. | 7 |
| 2.4 | The Guggenheim plot | 9 |
| 3.1 | The Migdal–Kadanoff spin-decimation | 16 |
| 3.2 | The RG transformation applied to a triangular lattice proposed by Niemeijer and Van Leeuwen. | 18 |
| 4.1 | Relative positions of atoms for the types of orders corresponding to each fixed point. | 32 |
| 4.2 | Phase diagram for the isotropic tetrahedral Ising lattice | 34 |
| 4.3 | The critical surface for the anisotropic tetrahedral Ising lattice as a result of the RG analysis with $J_1 = J_2 > 0$ | 35 |
| 4.4 | The topology of the critical surface | 35 |

List of Tables

| | | |
|-----|---|----|
| 2.1 | Maxwell relations among the thermodynamic parameters of a magnetic system | 4 |
| 2.2 | Critical exponents and related thermodynamic quantities. | 10 |
| 2.3 | “Scaling laws” relating the critical exponents | 11 |
| 3.1 | The critical exponents in terms of y_t and y_h | 19 |
| 4.1 | Ordered phases of interest | 27 |
| 4.2 | Spins that form a block | 27 |
| 4.3 | Comparison of results of this work with established results . . . | 31 |
| 4.4 | Symmetries of the Hamiltonian | 33 |

Chapter 1

INTRODUCTION

Quantum mechanics along with the relativistic corrections in principle draws a complete picture of the universe, in the sense that once the rules governing the dynamics of individual particles are set, one can predict the behavior of any collection of particles, however complicated it is. Unfortunately, this approach fails to produce any solvable model when one has to deal with a macroscopic system with practically infinite degrees of freedom. So we need some extra tools which will carry the microscopic world of atoms to our kitchen. Statistical mechanics enters the picture right at this point: formulating the collective behavior of a cluster with $\sim 10^{23}$ particles.

Development of statistical mechanics starts in the second half of the 19th century with the pioneering studies of the scientists of the time like J. Clerk Maxwell, J. Willard Gibbs, Ludwig Boltzmann, Thomas Andrews and Rudolf Clausius on thermodynamic properties of matter. They investigated new laws of physics relating the thermodynamic variables such as pressure, volume and temperature which are experimentally measurable, plus some new quantities such as internal energy and entropy, though unmeasurable, proved to be essential parameters in determining the equilibrium state of a given system. However, soon physicists faced a real challenge in the investigation of the response of a macroscopic system to a change in the environment. That is, many systems exhibit an abrupt change of character at a critical value of an external variable, such as temperature or magnetic field, which varies in a perfectly smooth manner throughout a given interval. In other words, when the time comes, all the particles simultaneously decide to behave differently than they used to do. This anomalous behavior, namely *phase transitions* in many physical systems will be our main point of interest from now on.

There is a diverse collection of physical systems that undergo phase transitions in various forms giving a first impression as if it is unlikely that a general theory can be built. Some examples are liquid-gas transition of many materials, superfluidity of liquid helium, spontaneous magnetization of spin systems, order-disorder transition in binary alloys and superconducting transition of some metals and ceramics. Though the physical laws governing each one of the above transitions are quite unrelated, there are certain underlying similarities giving the clues of a unification. Chapter 2 will present the earlier theories of phase transitions and the appearance of a unified picture through the ideas of scaling. The modern approach to the critical phenomena is based on Renormalization Group ideas introduced by K. Wilson and developed further by L.P.Kadanoff, M.E. Fisher, B. Widom and many others. The physical grounds of the theory and its technical aspects will be given in Chapter 3. In Chapter 4, a new Kadanoff blocking scheme applicable to tetrahedrally structured systems will be proposed. The model allows for a possible anisotropy in one of the bond directions and is expected to be applicable to SiGe superlattices in which a new order-disorder transition has recently been observed. The resulting phase diagram for the tetrahedral Ising lattice will be analyzed in the same chapter.

Chapter 2

PHASE TRANSITIONS AND CRITICAL PHENOMENA

Equilibrium statistical properties of a system with many degrees of freedom are given in terms of its, so called, *Partition Function* (or *Zustandsumme*, German word meaning -the great sum-). It is a measure of the volume occupied by the set of all possible states in the phase-space. For a classical system, this is equivalent to a sum (or an integral for continuous degrees of freedom) of the corresponding Boltzmann factors over all possible configurations as below :

$$Z = \sum_{q_1=1}^{N_1} \sum_{q_2=1}^{N_2} \cdots \sum_{q_n=1}^{N_n} \exp^{-\beta H(q_1, \dots, q_n)} \quad (2.1)$$

where $\beta = 1/kT$, k being the Boltzmann constant and T the temperature and each coordinate q_i can take N_i discrete values. Instead of Eqn.2.1, one generally uses the shorthand notation below :

$$Z = \sum_{\{q_i\}} \exp^{-\beta H(q_i)}$$

Once the partition function is defined and computable, the corresponding Helmholtz Free Energy can be written down as

$$F = - \ln Z / \beta \quad (2.2)$$

and remaining thermodynamic quantities follow immediately from the Maxwell relations, e.g. for a magnetic system as in Table 2.1. Corresponding relations

Table 2.1: Maxwell relations among the thermodynamic parameters of a magnetic system

| | | | |
|--------------------------------|----------|-----|-----------------------------------|
| Average magnetization | M | $=$ | $-(\partial G/\partial H)_T$ |
| Magnetic field | H | $=$ | $-(\partial F/\partial M)_T$ |
| Specific heat of magnetization | C_M | $=$ | $-T(\partial^2 F/\partial T^2)_M$ |
| Isothermal susceptibility | χ_T | $=$ | $-(\partial^2 G/\partial H^2)_T$ |

for a fluid may be obtained by the following substitutions :

$$\begin{array}{lcl} H & \longrightarrow & P \\ M & \longrightarrow & -V \end{array} ,$$

A phase transition manifests itself as an anomaly in the behavior of these equilibrium properties in response to an external field, for example the temperature. The transition from one thermodynamic state to another may demonstrate qualitative differences depending on whether the transition is of *1st* or *2nd* order. The distinction between the two is made by observing the behavior of the free energy at the transition point (after Ehrenfest). The first order transitions display a discontinuity in the *1st* derivative of the Gibbs free energy, or equivalently in the entropy, whereas the discontinuity of a second order transition is by definition in the second or higher derivatives (see Fig.2.1)

First order phase transitions have been known for centuries, the most common examples being the liquid-gas, solid-liquid and solid-gas transitions of a given substance.

The graphical demonstration of the equilibrium state properties according to changing ambient parameters is known as a **phase diagram**. Consider for instance solid-liquid-gas phase diagram of water in Fig.2.2.

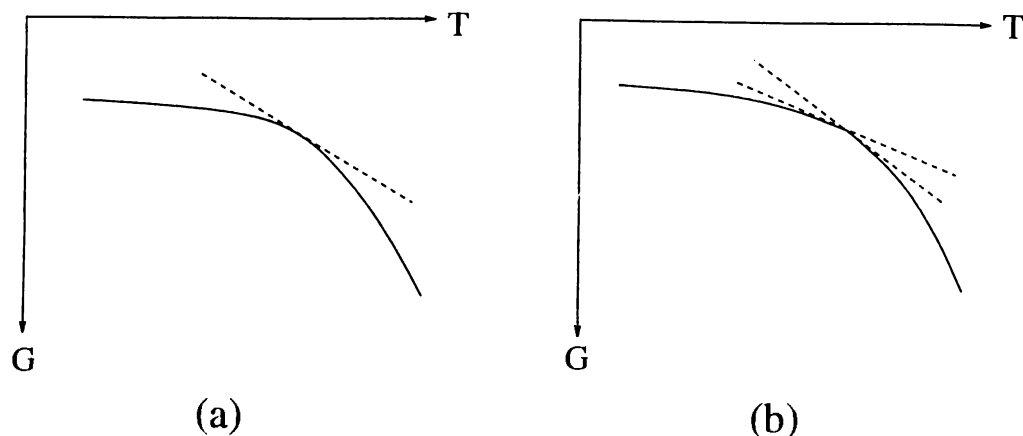


Figure 2.1: Behavior of the free energy of the system in (a) 2nd and (b) 1st order phase transitions

The phase boundaries are in fact the curves of coexistence representing the equilibrium states in which two phases with *different* densities survive simultaneously. As a consequence, at the tricritical point all three phases coexist (for water $P_t = 218 \text{Atm}$, $T_t = 374^\circ \text{C}$ [1]). The system exhibits its criticality (in the sense of statistical mechanics) at the point (T_c, P_c) where the liquid-gas coexistence curve terminates. The meaning of termination is, above this point the density difference between the two phases vanishes and the phase transition along path (2) is of *second order*. Disappearance of the density difference is an example of a characteristic feature of second order phase transitions, namely vanishing of a parameter -called the **order parameter**- above the critical point, marking the onset of a previously absent symmetry. Another indicator of second order phase transitions is the divergence of a number of thermodynamic functions such as the specific heat (as in λ - transition of liquid helium), susceptibility, correlation function and the correlation length at the critical point. Among these, divergence of the correlation length introduces the fact that at T_c all the physical lengths vanish tending to either 0 or ∞ (this will be discussed in Chapter 3). There exist fluctuations of all sizes. This induces an exotic phenomenon known as the *critical opalescence* in certain liquid-gas phases and binary mixtures. That is, at the criticality, the substance - otherwise transparent - bears a white, cloudy appearance thanks to the domains of the size of several thousand atoms which scatter visible light appreciably.

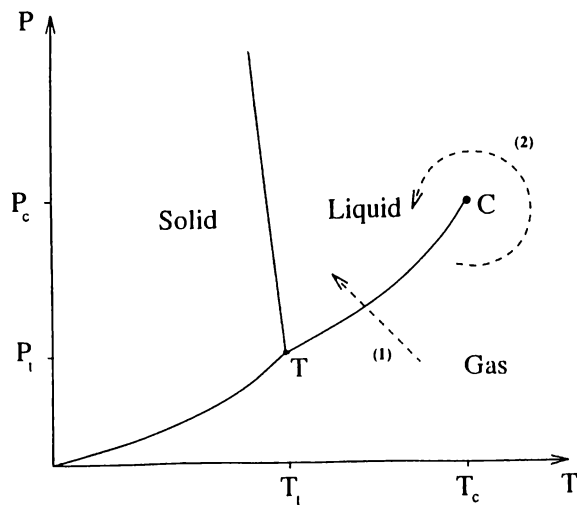


Figure 2.2: Phase diagram of water. T is the triple point where three phases coexist and C is the critical point. (1) and (2) indicate paths along which the transition is of 1st and 2nd order respectively.

2.1 A Review of History

The existence of such a critical point was first reported by Andrews for CO_2 in his famous article titled “On the continuity of the gaseous and liquid states of matter” [2]. After four years, Van der Waals made the first theoretical attempt for the combination of liquid and gas states of matter in a single theory. He published his well-known equation of state in his PhD thesis titled “On the continuity of gaseous and liquid states” [3]. Strangely enough, he was completely unaware of Andrews’ work at that time. For a historical review, see for example [4, 5, 6]. The second order phase transition in magnets was first formulated by Weiss in 1907 [7]. The transition occurs at Curie temperature T_c and zero external magnetic field by the appearance of a self magnetization. The magnetization defines a preferred direction in space, destroying the rotational invariance of the system (see Fig.2.3). This phenomenon is called *spontaneous symmetry breaking*. Note that the self magnetization for the magnet is what density difference to the liquid–gas system is, i.e. the **order parameter**. The necessity of an extra parameter to define the thermodynamic state below T_c eliminates the possibility of representing the system with a single analytic function of thermodynamic variables on both sides of the critical point. Here appears a puzzle for, the partition function being a sum of analytic terms is itself also expected to be analytic. So how does the non-analyticity arise? Answering this question has been the main challenge in the field of critical phenomena but a complete theory is still lacking. An immediate observation is that the partition function can have a non-analyticity only when the number of

terms in Eqn.2.1 tends to infinity. So from this simple discussion, we reach the important conclusion that criticality formally exists only in the thermodynamic limit, i.e. $V \rightarrow \infty$, $N \rightarrow \infty$, with N/V constant.

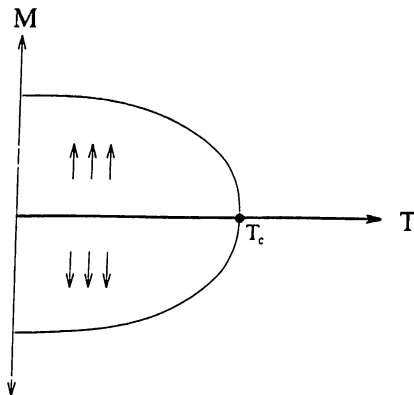


Figure 2.3: Phase diagram for an Ising ferromagnet at the critical external magnetic field $H = 0$. Below the Curie temperature T_c , rotational symmetry is destroyed by the appearance of a nonzero magnetization.

2.1.1 Landau Mean Field Theory

In 1937, Landau proposed what is now called the *Landau Mean Field Theory* (LMFT) [8] as a theoretical ground for studying critical phenomena. His theory covered Van der Waals' and Weiss' formulations as special cases and was able to predict the behavior of the thermodynamic properties at the critical point. LMFT is so simple that a few lines can be spent to show how it works, e.g. for a magnet. Landau assumes the free energy F is an analytic function of the average magnetization M , so that for $H_{ext} = 0$, one can express F as a Taylor expansion in powers of M for small values of M :

$$F(M, T) = G_0(T) + a(T)M^2 + b(T)M^4 + \dots \quad (2.3)$$

Note that only even powers of M contribute to F because of the up-down symmetry in the absence of external field. To find the actual F , one minimizes (2.3) with respect to M :

$$\frac{\partial F}{\partial M} = 2a(T)M + 4b(T)M^3 + \dots = 0 \quad (2.4)$$

Now truncate (2.4) with the first two terms and assume $b > 0$. Since $\partial F / \partial M = H$ by Maxwell relations given above, this condition guarantees that H increases with M when M is large. For $a > 0$, G has a single minimum at $M = 0$. However, if $a < 0$, G has two minima at $M = \pm \sqrt{-a/2b}$ which suggests that $a > 0$ corresponds to $T > T_c$ and $a < 0$ corresponds to $T < T_c$. Further assume

that a and b are analytic functions of T so that to the first approximation, b is a constant and $a \propto (T - T_c)$. So LMFT predicts

$$M \propto (T_c - T)^{1/2} \quad (2.5)$$

around $T = T_c$. Consequently, by Eqn.2.4,

$$\chi = \partial M / \partial H = \frac{1}{2a} \propto (T - T_c)^{-1}$$

for small M . The exponents $1/2$ and -1 are now given certain names (β and $-\gamma$ respectively) for reasons that will become clear later (see Table 2.2).

2.1.2 Experiment Conflicts Theory

In 1893, Van der Waals had also obtained a similar expression from the asymptotic behavior of his equation at the critical point [9]. He analyzed the volume difference of the liquid (+) and gas (-) phases in the two-phase region and got

$$V^\pm - V_c = \mp B_1 |T - T_c|^{1/2} + B_2 |T - T_c| + \dots$$

from which Van Laar in 1912 [10] derived

$$\rho^\pm - \rho_c = B_1 |T - T_c|^{1/2} \quad (2.6)$$

for $T \sim T_c$. Note that Eqn.2.6 is dual to Eqn.2.5 since both terms on the left are the order parameters of the corresponding system. A few years later however, controversial experimental results started being reported [11, 12, 13, 15]. Numerous experiments with increasing sensitivity showed that β was closer to $1/3$ rather than the theoretical prediction $1/2$. A similar problem existed for the other exponents, too. So, the underlying physics of the critical phenomena had to be different from Van der Waals' theory. Something was obviously going wrong and nobody knew what it was.

2.2 Universality and Scaling Laws : The Modern Era

2.2.1 Law of Corresponding States

The non-analytic behavior of a substance at criticality, either as the divergence of specific heat and susceptibility or as the sudden appearance of magnetization possesses qualitative and quantitative similarities in many unrelated physical systems. Guggenheim plot Fig.2.4 is a classical example of independence of the shape of the coexistence curve from the substance in a liquid-gas tran-

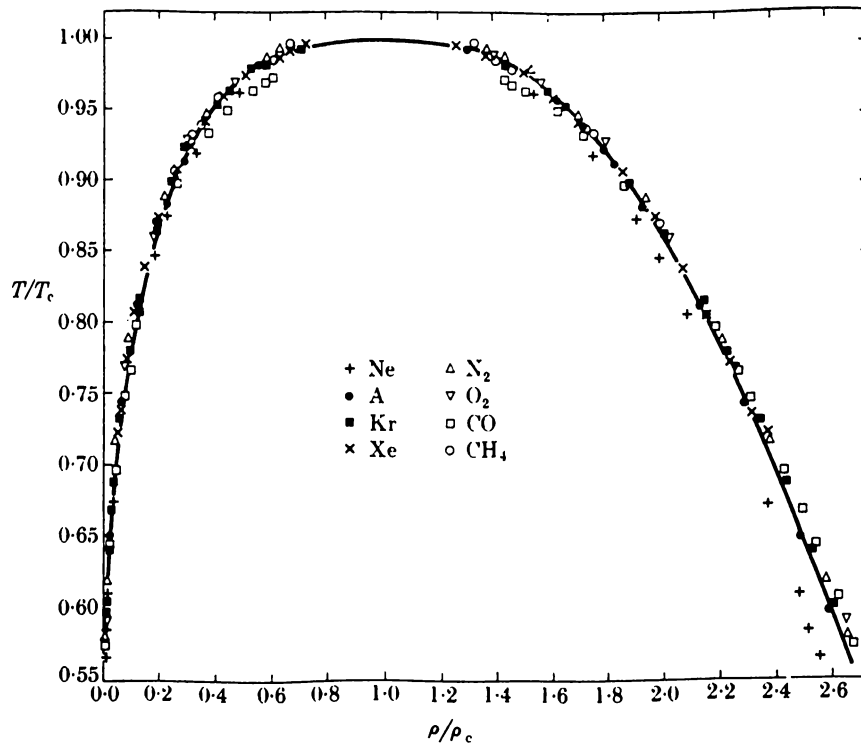


Figure 2.4: The famous Guggenheim plot showing the coexistence curves for the eight fluids indicated (from Stanley [14]).

sition. This likeness continues further in magnetic systems. Consider the magnetization curve in Fig.2.3.

It was again Van der Waals in 1880 [16] who came out with the idea that the vapor pressure curves of all substances should be the same when they are represented in terms of rescaled quantities as $\pi = p/p_c$, $\phi = V/V_c$ and $\theta = T/T_c$ such that

$$\pi = \pi(\phi, \theta).$$

Then, states of different substances could be given by the above single equation involving these variables and same π , ϕ and θ would represent the **corresponding states** for different substances. This proposition carried a great importance, because it allowed one to derive the properties of an unknown material by simply looking at its critical parameters. Then the equation of state could be predicted from that of a previously studied sample. Later, Kamerlingh Onnes [17] generalized the “law of corresponding states” and restated the idea in terms of molecular interactions, i.e. defining as two basic parameters a characteristic size and an interaction strength for each substance. Consequently, the corresponding states were derivable using proper scalings involving these two quantities.

The **law of corresponding states** is a statement of universality which is closely linked to a more recent observation on critical phenomena which can be stated as follows :

The critical (nonanalytic) behavior of a system can be expressed by power laws using certain exponents which are independent of the specific Hamiltonian defining its physical properties. These exponents depend merely on the dimensionality of the system and on the degrees of freedom of its constituents.

2.2.2 Critical Exponents and Scaling Laws

The nonanalytic behavior of many physical properties near the point of criticality is given by certain exponents independent of the Hamiltonian describing the specific system. These are called the *critical exponents* and they play a key role in modern theories of criticality. A list of these exponents and the corresponding parameters is given in Table 2.2.

| <i>Exponent</i> | <i>Definition</i> | <i>Quantity in fluid (magnetic) systems</i> |
|-----------------|---------------------------------------|---|
| α | $C \sim t ^{-\alpha}$ | Specific heat at const. volume (magnetic field) |
| β | $\rho_L - \rho_G (M) \sim (-t)^\beta$ | Density difference (zero-field magnetization)* |
| γ | $\chi \sim t ^{-\gamma}$ | Isothermal compressibility (susceptibility) |
| ν | $\xi \sim t ^{-\nu}$ | Correlation length |
| η | $\Gamma(r) \sim r ^{-(d-2+\eta)}$ | Pair correlation function ($t=0$) |
| δ | $M \sim H^{-1/\delta}$ | Critical isotherm ($t=0$) |

*Valid only for $T < T_c$ by definition of order parameter.

Table 2.2: Critical exponents and related thermodynamic quantities. Let $t = (T - T_c)/T_c$

The numerical values of these very special exponents are either known by the exact solution of certain model Hamiltonians, or approximated by several expansion techniques or numerical simulations – sometimes in specially designed hardware – and of course by experiments. However, these exponents

| | | | |
|----------------------------|-----|---------------------|-------------------|
| γ | $=$ | $\nu(2 - \eta)$ | (Fisher,[18]) |
| $\alpha + 2\beta + \gamma$ | $=$ | 2 | (Rushbrooke,[19]) |
| γ | $=$ | $\beta(\delta - 1)$ | (Widom,[20]) |
| νd | $=$ | $2 - \alpha$ | (Josephson,[21]) |

Table 2.3: “Scaling laws” relating the critical exponents

are not all linearly independent : if only two of them are known, the rest can be derived using certain “scaling laws”. The immediate question is “Why two?”. A satisfactory, though not rigorous, answer to this question regarding “Widom hypothesis” is presented in Chapter 3. Nevertheless, it is informative to illustrate here how these relations can be derived through physical arguments. A basic postulate of the theory of criticality is that near the critical point, the correlation length ξ is the only relevant length scale in terms of which all quantities with the dimensionality of length should be measured. This is known as the **scaling hypothesis**. Now if we assume the pair-correlation function to have the Ornstein-Zernike form

$$\Gamma(\mathbf{r}) = \exp^{-|\mathbf{r}|/\xi} / |\mathbf{r}|^{d-2+\eta},$$

then at the critical point $\Gamma \sim (\text{length})^{-(d-2+\eta)}$. Using the scaling hypothesis and the definition $\xi \sim |t|^{-\nu}$,

$$\Gamma \sim |t|^{\nu(d-2+\eta)}.$$

However, by the fluctuation-dissipation theorem,

$$\chi = \frac{1}{kT} \int d^d x \Gamma(\mathbf{r})$$

so that $\chi \sim |t|^{-\nu(2-\eta)}$. This gives the well-known “Fisher law” :

$$\gamma = \nu(2 - \eta).$$

Several scaling laws relating the exponents previously defined in Table 2.2 are listed in Table 2.3.

A deeper understanding of these relations through a unified point of view is provided by Kadanoff’s scaling picture. In Chapter 3, the origins and the physical meaning of scaling, Kadanoff’s revolutionary theory and its implications will be discussed.

Chapter 3

RENORMALIZATION GROUP

The problem of critical phenomena needs a careful treatment, because one can not use a perturbative approach in treating the fluctuations at irrelevant scales since all scales are relevant. This exactly is the reason why the classical mean-field theories fail at the point of criticality. A successful theory would be the one that considers all energy or length scales on an equal footing and the one that is universal enough to be applicable to a variety of problems with the same handicap. In this chapter, the **Renormalization Group (RG)** will be presented as such a technique for exploring the region of criticality. It appears to be a natural approach to problems involving scale invariance for the procedure it proposes is a *rescaling* of momentum or position space dimensions.

The key idea of RG is to transform the original Hamiltonian into another form and thereby to thin out the degrees of freedom within dimensions of a correlation length. This is a repeated scaling transformation where at each step the components of the new system are obtained by an averaging over short wavelength fluctuations. Naturally, there are some restrictions on this transformation. First, all physical properties should be conserved throughout the whole process. This can be achieved only by keeping the Partition function unchanged at each step. Furthermore, the mapping should preserve the space dimensionality (d) and the spin degrees of freedom (n), which are the only parameters that define the universality class of the critical behavior under exploration. This is because, every new Hamiltonian is merely another representation of the original system with a definite d and n . Finally, not a formal but technical restriction is that the transformation should not create new types of interactions absent in the previous Hamiltonian, since otherwise it would not be practical to apply it repeatedly. So the RG transformation has a cascade structure with $H_{l+1} \equiv \mathfrak{R}\{H_l\}$ and defines a flow for every point in

the space of Hamiltonians. The unique geography of the space of Hamiltonians determined by the RG flows tells the critical behavior of our model. That this geography is independent of the original coordinates of H_0 is nothing but the statement of the universality discussed in Chapter 2.

Apart from critical phenomena, the RG theory has found applications in a variety of fields including Quantum electro-dynamics, Quantum chromo-dynamics, percolation theory, the Kondo problem, turbulence and polymer physics.

3.1 Momentum-Space Renormalization

The origin of RG is quantum field theory of elementary particles where one usually has to compute sums over intermediate states with energies starting from mc^2 up to infinity. These computations generally end up with a logarithmic divergence of the form $\int_{mc^2}^{\infty} dE/E$ (ultraviolet divergence). This is an indicator of the lack of a characteristic energy scale in the problem. The standard renormalization procedure was developed first by Schwinger, Bethe, Feynman, and Dyson to remove the divergences in the theory. Later Wilson and Kogut, pointing out the similarity between the divergences observed in Quantum Field Theory and Statistical Mechanics (except that the ultraviolet limit of Quantum Field Theory is changed to infrared in Statistical Mechanics), proposed a RG scheme applicable to critical phenomena [22].

As a suitable ground for discussing this technique, consider for example a d -dimensional spin lattice with spin s_i sitting on the i -th site according to a suitable indexing. Given s_i , one can define an average magnetization $M(x)$ for the $1/\Lambda$ neighborhood of x as

$$M(x) = \int_0^\Lambda M_k \exp\{-i \mathbf{k} \cdot \mathbf{x}\} d\mathbf{k} \quad (3.1)$$

so that fluctuations within regions of size $\sim 1/\Lambda$ do not change $M(x)$ much (M_k is the Fourier transform of s_i). Thereby, one can define an effective Hamiltonian in terms of M_k :

$$\exp\{H_\Lambda(M)\} = \sum_{\{s_i\}} \left\{ \prod_{k=0}^\Lambda \delta(M_k - \sum_n \exp\{i \mathbf{k} \cdot \mathbf{n}\} s_i) \right\} \exp\{-H_0/kT\}. \quad (3.2)$$

Note that the Partition function for the new Hamiltonian is equal to the original Partition function, i.e.,

$$Z = \sum_{\{s_i\}} \exp\{-H_0/kT\} = \prod_{k=0}^{\Lambda} \int_{-\infty}^{\infty} dM_k \exp\{H_{\Lambda}(M)\}. \quad (3.3)$$

One has to be careful when dealing with an infinite lattice, because the multiplication over discrete \mathbf{k} vectors in Eqn.3.3 becomes a functional integration which needs a careful treatment. However, we will skip it here and assume that the lattice is finite.

Now we can write down the RG transformation as a relation between $H_{\Lambda/2}$ and H_{Λ} . We do this by integrating the short wavelength fluctuations with $\Lambda/2 < k < \Lambda$ and keeping the Partition function unchanged (1/2 is an arbitrary choice) :

$$\exp\{H_{\Lambda/2}(M)\} = \prod_{k=\Lambda/2}^{\Lambda} \int_{-\infty}^{\infty} \exp\{H_{\Lambda}(M)\} dM_k \quad (3.4)$$

apart from a constant factor. By substituting dimensionless momentum and scaled magnetization $\mathbf{q} = \mathbf{k}/\Lambda$ and $\sigma_{\mathbf{q}} = M_{\mathbf{k}} \cdot \alpha_{\Lambda}$ Eqn.3.4 becomes

$$\exp\{H_{\Lambda/2}(\sigma')\} = \prod_{|\mathbf{q}|>1/2}^1 \int_{-\infty}^{\infty} \exp\{H_{\Lambda}(\sigma)\} d\sigma_{\mathbf{q}}. \quad (3.5)$$

Eqn.3.5 is the final form of momentum-space RG transformation proposed by Wilson [23]. Let us denote it as $H_{\Lambda/2} = \mathfrak{R}\{H_{\Lambda}\}$. The aim in introducing σ and \mathbf{q} is to make possible the existence of a fixed point of the transformation for the reason discussed below.

Eliminating a momentum scale and then rescaling the momenta (so that $0 < |\mathbf{q}| < 1$), it can be shown that one defines a new lattice where the correlation length is also scaled as $\xi_{\Lambda/2} = \xi_{\Lambda}$. Then we can expect the *fixed points* of the RG transformation to give hints about the behavior of our system around criticality where $\xi \rightarrow \infty$. Because, if there is an H^* such that $H^* = \mathfrak{R}\{H^*\}$, then $\xi_{\Lambda/2} = \xi_{\Lambda}$ which forces $\xi = 0$ or $\xi = \infty$. First is the trivial fixed point and is of little interest, but the latter refers to the critical point and deserves careful analysis.

Actually, the non-trivial fixed point usually cannot be calculated exactly. Therefore, under certain analyticity assumptions which are valid in restricted cases, $H(\sigma)$ is assumed to have a power series expansion for small σ and is approximated by the leading terms in the expansion. The number of non-trivial fixed points (there can be more than one) and the value of the calculated critical exponents depend on the approximations made after this point. Mean-field results correspond to the first-order approximation in this formulation.

There are perturbation expansions such as the ε -expansion and $1/n$ -expansion which are built on this renormalization scheme (n : spin degrees of freedom). The success of such expansions is due to the fact that the problem becomes trivial in the limit $d \rightarrow 4$ or $n \rightarrow \infty$ [22, 24].

3.2 Position-space Renormalization

That the fluctuations can be integrated one scale at a time in position-space was first proposed by Kadanoff [25]. Later on, Kadanoff's block-spin method was extensively studied and applied to several model systems with success [26, 27], see also [28]. Specially, in two-dimensional models where the ε -expansion and $1/n$ -expansion fail, block-spin methods can work surprisingly good. Although the Ising square lattice with nearest-neighbor interaction is exactly solvable [29] and does not need a RG treatment, the solution applies only to a restricted class of models in two-dimensions. The Monte Carlo RG is a later method proposed by Swendsen [30] and is applicable to two and three-dimensional models with relative ease (see also [31, 32]).

3.2.1 Spin-decimation method

Consider the Partition function for a two-dimensional Ising ferromagnet with zero external magnetic field

$$Z = \sum_{\{s_n\}} \exp \left\{ K \sum_n \sum_i s_n s_{n+\hat{i}} \right\} \quad (3.6)$$

where \hat{i} denotes the unit vector in the direction \mathbf{i} . The number of terms in the sum grows exponentially with the dimension of the lattice, i.e. for an $N \times N$ square lattice we have 2^{N^2} terms. Moreover, the analysis of critical phenomena necessitates N to be large, because one has to consider a lattice of macroscopic size as $\xi \rightarrow \infty$. The straight-forward evaluation of the sum is a hopeless task.

Instead, the sum can be evaluated partially over (e.g.) half of the spins with relative ease and this can be repeated successively over the remaining spins. This is the ‘‘Migdal-Kadanoff spin-decimation’’. For example, consider the square lattice in Fig.3.1. Take the partial sum over ‘ x ’ spins keeping ‘ o ’ spins

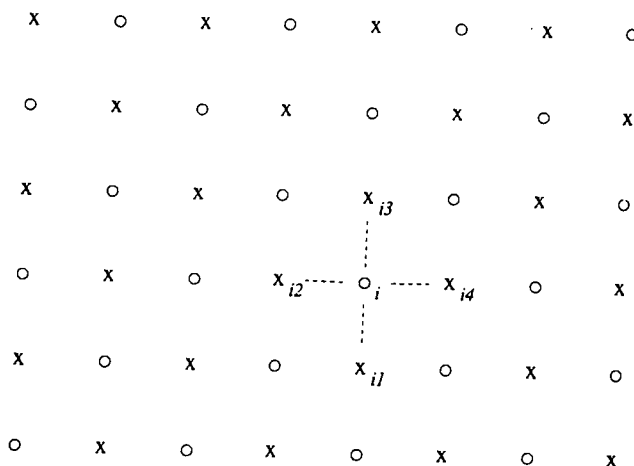


Figure 3.1: The spin-decimation method applied to a square lattice. 'o' spins are kept fixed and the Partition function is summed over the 'x' spins.

fixed. The sum will be a function of 'o' spins only. Assign a new Hamiltonian $H'(o)$ to the 'o-lattice' s.t.

$$\exp\{H'(o)\} = \sum_{\{x_i\}} \exp\left\{K \sum_i x_i (o_{i1} + o_{i2} + o_{i3} + o_{i4})\right\}. \quad (3.7)$$

It is obvious that the Partition function is unchanged with this transformation. Since all nearest-neighbors of 'x' spins are 'o' spins, the sum in Eqn.3.7 can be factorized as

$$\begin{aligned} \exp\{H'(o)\} &= \prod_i \sum_{x_i = \pm 1} \exp\{K x_i (o_{i1} + o_{i2} + o_{i3} + o_{i4})\} \\ &= \prod_i 2 \cosh[K(o_{i1} + o_{i2} + o_{i3} + o_{i4})] \\ &= \exp\{A(K) + B(K) \sum_{j \neq k} o_{ij} o_{ik} + C(K) o_{i1} o_{i2} o_{i3} o_{i4}\} \end{aligned} \quad (3.8)$$

where the final substitution uses $\cosh(x) = \cosh(-x)$. H' which applies to the new square lattice with half the spins turns out to be

$$\begin{aligned} H'(s) &= A(K) + \sum_n \sum_i 2 B(K) s_n s_{n+i} + \sum_n \sum_{\pm} B(K) s_n s_{n+i \pm 2} + \\ &\quad \sum_n C(K) s_n s_{n+i} s_{n+2} s_{n+i+2} \end{aligned} \quad (3.9)$$

Unfortunately, H' includes interactions which are absent in H_o . This eliminates the possibility of an exact RG transformation because the third and fourth terms in H' couple two 'x' spins in the new lattice and the new Partition function can not be decoupled. In a practical construction of an RG

transformation, one generally comes to such a decision point where a suitable approximation has to be made in order to proceed (though there *are* very exceptional two-dimensional models on which an exact differential RG transformation is definable [33]). See [32] for more about spin-decimation method.

Although the Migdal-Kadanoff transformation is very favorable for its simplicity and applicability in all dimensions, it has a well-known unphysical consequence [34] : The spin-spin correlation function $\Gamma_H(r)$ transforms as

$$\Gamma_H(r) = \Gamma_{H'}(r/2) \quad (3.10)$$

where r is measured in terms of the lattice spacing. But this transformation does not allow the expected critical behavior $\Gamma_H(r) \sim |r|^{-(d-2+\eta)}$ in systems where $d-2+\eta \neq 0$. This inconsistency is claimed to be the reason for the bad performance of the transformation in predicting the critical exponent ν .

3.2.2 Kadanoff's Block-Spin Method

There's a simpler way of realizing the idea of Wilson's momentum-space RG in position-space. An RG transformation can be set by constructing blocks from a group of spins as in Fig.3.2, then treating the blocks as single spin variables and building an effective Hamiltonian coupling the block-spins. If the new spin lattice bears the same symmetries with the original, then a scaling transformation maps the blocks onto the original lattice sites. The block-spin variables display the average effect of their internal components, but do not carry as detailed information. Therefore, the short range fluctuations are effectively averaged out and the long wavelengths which are dominant at the critical point are kept. A sample transformation first proposed by Niemeijer and Van Leeuwen [26] is shown in Fig.3.2. The spin values of the blocks are decided by the majority law :

$$\begin{aligned} s' &= \text{sgn}(s_1 + s_2 + s_3) \\ &= \frac{1}{2} (s_1 + s_2 + s_3 - s_1 s_2 s_3) \quad , \quad s_i = \pm 1 \end{aligned} \quad (3.11)$$

which is again either $+1$ or -1 . The block Hamiltonian is defined as follows :

$$K \exp \{ H'(s') \} = \sum_{\{s\}} p(s'; s) \exp \{ H(s) \} \quad . \quad (3.12)$$

The kernel $p(s'; s)$ is $+1$ if its arguments satisfy Equ.3.11 and 0 otherwise. It

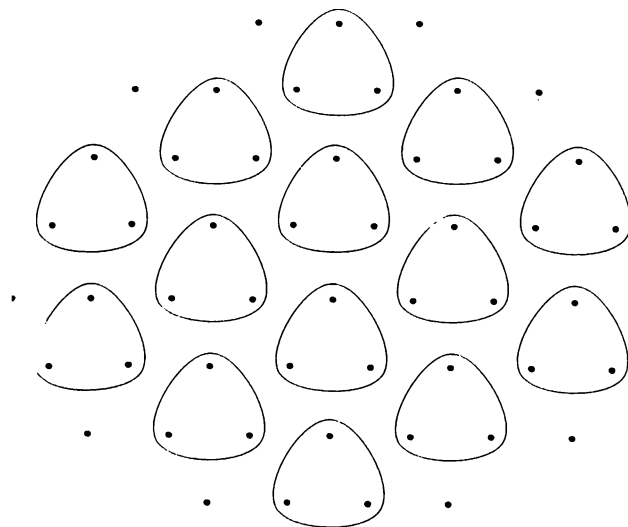


Figure 3.2: The RG transformation applied to a triangular lattice proposed by Niemeijer and Van Leeuwen.

is called the *projection operator*. The completeness relation

$$\sum_{\{s'\}} p(s'; s) = 1$$

guarantees that the Partition function is conserved. The constant factor K on the LHS of 3.12 stores the extra free energy throughout the transformation. Finally we need to scale every length in the primed-lattice by $\sqrt{3}$ so that the lattice spacing remains the same. So the two crucial steps are the choice of the blocks and the projection operator. The projection operator $p(s'; s)$ does not necessarily correspond to a majority rule. There are alternative choices offered to avoid inconveniences due to forcing the block spin to be ± 1 (e.g. see [35, 36]).

3.2.3 Scaling Hypothesis and Critical Exponent Relations

RG analysis offers an alternative picture for the linear dependence of the critical exponents defined in Chapter 2. Consider an RG transformation with a scaling constant L ($L = \sqrt{3}$ for the previous example) and let $f(t, H)$ represent the singular part of the free energy density where $t = (T - T_c)/T_c$ and H is the external magnetic field. After a single RG step, the correlation length will shrink by a factor L . So we will move further apart from the critical point. The new free energy density will satisfy

$$f'(t', H') = L^d f(t, H)$$

| | | | | | |
|--------------|-----|-----------------|----------|-----|------------------|
| $2 - \alpha$ | $=$ | d/y_t | γ | $=$ | $(2y_h - d)/y_t$ |
| $1/\delta$ | $=$ | $d/y_h - 1$ | ν | $=$ | $1/y_t$ |
| β | $=$ | $(d - y_h)/y_t$ | η | $=$ | $d - 2y_h + 2$ |

Table 3.1: The critical exponents can be expressed in terms of y_t and y_h which are obtained from the relevant eigenvalues of the linearized RG transformation.

because the new spin crystal with its own t' and H' is merely another representation of the original system. Remember that the Partition function is not changed. At this point, we make an assumption known as “Widom Hypothesis” [37]:

Since we move away from the criticality, t and H may also scale by some powers of L , i.e.

$$L^d f(t, H) = f(L^{y_t} t, L^{y_h} H) \quad \forall L \quad y_t, y_h > 0$$

or in the language of mathematics, $f(t, H)$ is a generalized homogeneous function. The quantities y_t and y_h are two positive (since the system becomes less critical) exponents scaling the temperature and the magnetic field, i.e. the symmetry breaking fields. Without loss of generality, one may choose $L = H^{-1/y_h}$ or $L = t^{-1/y_t}$ to get

$$\begin{aligned} f(t, H) &= H^{d/y_h} f(t \cdot H^{-y_t/y_h}, 1) \\ &= t^{d/y_t} f(H \cdot t^{-y_h/y_t}, 1) \end{aligned} \tag{3.13}$$

Using Eqn.3.13, Table 2.1 and Table 2.2, listed critical exponents can be expressed in terms of y_t , y_h and d (see Table 3.1). Specifically, ν and η which are functions of y_t and y_h only are a good basis for expressing all critical exponents (see Table 2.3). In this picture, there exist naturally two linearly independent exponents, because temperature and the magnetic field are the only *relevant* parameters affecting the criticality. The meaning of “relevant parameter” and the role of relevant and irrelevant parameters in the theory of critical phenomena will be discussed in the next section.

3.3 Linearized RG transformation

Consider the RG flow $H_{l+1} = \mathfrak{R}\{H_l\}$ and a non-trivial fixed point $H^* = \mathfrak{R}\{H^*\}$. By the continuity of the flow, if H_l is close to H^* , then H_{l+1} should also be close to H^* . Then, if

$$H_l = H^* + \delta H_l,$$

then \mathfrak{R} can be approximated by a linear transformation

$$\mathfrak{R}\{H_0\} = \mathfrak{R}\{H^* + \delta H_0\} \simeq \mathfrak{R}\{H^*\} + \mathcal{B} \delta H_0.$$

Terms of order $(\delta H_0)^2$ and higher are ignored. Now consider the eigenvalue problem below :

$$\mathcal{B}\mathcal{O} = \lambda\mathcal{O}$$

As a special case, if $\delta H_0 = \mathcal{O}$, then $\delta H_l = \lambda^l \mathcal{O}$. More generally, if $\{\mathcal{O}_i\}$ make a complete set, then δH_0 can be expressed as a linear combination of them :

$$\delta H_0 = \sum_i \mu_i \mathcal{O}_i \Rightarrow \delta H_l = \sum_i \mu_i \lambda^l \mathcal{O}_i. \quad (3.14)$$

Strictly speaking, validity of such an expansion is not always guaranteed for several reasons. First, if \mathcal{B} is not Hermitian, RHS of Eqn.3.14 may include additional terms of the form $l^k \lambda_i^l$. We will assume that this is not the case. Second, \mathcal{B} is most generally an infinite dimensional matrix operating on vectors δH_l of an infinite dimensional interaction space including all n-body couplings. Therefore, the completeness of $\{\mathcal{O}_i\}$ is not guaranteed. However, in practice one can construct a \mathfrak{R} such that the same type of interactions are created at each step. Then, \mathcal{B} is $n \times n$ where n is the number of different couplings in H_0 .

Assuming λ_i 's are real (if not, below arguments are valid for $|\lambda_i|$), Eqn.3.14 hints the importance of eigenvalues greater than 1. If δH_0 includes an operator \mathcal{O}_r with $\lambda_r > 1$, δH_l will grow in each iteration with λ^l . H_l will move further and further away from criticality towards a trivial, non-critical fixed point. Such operators are called **relevant**. The number of relevant operators determine the number of parameters that must be fixed for criticality. For example, the criticality condition for a ferromagnet is $H = 0$ and $T = T_c$. That means we have only two relevant operators, call them \mathcal{O}_t and \mathcal{O}_H , responsible for the divergence from criticality with changing temperature or magnetic field. The critical exponents are found from the eigenvalues of the relevant operators.

The operators with $\lambda_i < 1$ are **irrelevant operators**, because their contribution to δH_l vanish in the limit $l \rightarrow \infty$. Their role in the theory of critical phenomena is central in the description of universality. For example, consider a critical Hamiltonian H_0 , i.e. $\lim_{l \rightarrow \infty} \mathfrak{R}^l \{H_0\} = H^*$. Let δH_0 be an infinitesimal perturbation to H_0 . Then corresponding H_l will also deviate from its original value : $H_l \xrightarrow{\mathfrak{R}} H_l + \delta H_l$. For large l , H_l is essentially H^* and δH_l can be linearized as in Eqn.3.14. If $H_0 + \delta H_0$ is also to be critical, then the coefficients μ_r of the relevant eigenvectors \mathcal{O}_r should be set to zero. This dictates a certain relation among the couplings existing in δH_0 . Note that $\{\mu_i\}$ is nothing but another representation of $H(\{K_i\})$ in a different basis. Apart from this relation, the details of the microscopic interactions in δH_0 do not effect the critical behavior.

Finally, there is a third type of eigenoperator for which $\lambda = 1$. These are the **marginal operators** and their contribution to δH_l neither increase nor decrease in the first order. Therefore, one has to go beyond the linear theory to decide on their relevance (see the RG treatment of the Kondo problem [23]). Existence of marginal operators may lead to a line of fixed points as in the case of Baxter model (see [47]). In this study, we will exclude the possibility of marginal operators.

3.3.1 Calculating ‘ ν ’

The critical exponents can be expressed in terms of the relevant eigenvalues. This calculation is important, because up to this point we could at best express the critical exponents in terms of y_t and y_h (see Table 3.1) which are still to be determined. However, if we have a RG transformation we can construct its linear model \mathcal{B} around H^* and extract its eigenvalues. Hence, RG is able to predict the critical exponents with a precision depending on the accuracy of the transformation.

Consider in the expression 3.14 the relevant operator related to the temperature and for simplicity assume that it is the only relevant operator of the transformation. Call it \mathcal{O}_t and the related eigenvector λ_t . Then H_l can be expressed as below :

$$H_l = H^* + \mu_t \lambda_t \mathcal{O}_t + \sum_i \lambda_i \mathcal{O}_i.$$

If H_0 is close enough to H^* then all μ_i 's (including μ_t) are $\ll 1$. Now consider an l_0 such that $|\mu_t| \lambda^{l_0} \sim 1$. For this value of l , the correlation length ξ_{l_0} will

have a fixed value regardless of the value of l_0 , because H_l will be fixed (last term in the above expression will be negligibly small). So that

$$\xi_{l_0} = L^{-l_0} \xi_0 = \text{const.} , \quad (3.15)$$

where L is the scaling constant of the RG transformation. Setting $\mu_l \lambda^{l_0}$ to unity along with Eqn.3.15 gives

$$l_0 = -\frac{\ln |\mu_l|}{\ln \lambda_r} \Rightarrow \xi_0 = (e^{\ln L})^{\ln |\mu_l| / \ln \lambda_r} \xi_{l_0}.$$

Assuming that μ_l is an analytic function of temperature and from the requirement that $\mu_l = 0$ at criticality, for $T \sim T_c$, $|\mu_l|$ should behave like $c|T - T_c|$. Then we can rewrite ξ_0 as

$$\xi_0 = \mu_l^{\ln L / \ln \lambda_r} \xi_{l_0} = |T - T_c|^{\ln L / \ln \lambda_r} \xi_{l_0}$$

so that $\nu = \ln L / \ln \lambda_r$. Note that ξ_{l_0} is just a constant factor.

3.3.2 Fixed points and critical surfaces

The topological arguments stated below help to visualize the structure of our RG transformation without using any algebra. We will ignore many possible complications and demonstrate only the basic ideas.

The RG trajectories, fixed points etc. define a certain geography in the space of Hamiltonians (S). S can be divided into one less dimensional subspaces where in each subspace ξ is constant. On a RG trajectory, the correlation length will decrease as $\xi(t) = e^{-t} \xi_0$, where t is the time parameter defining the velocity of the RG flow (for the discrete transformations we discussed so far, $t \sim l$). Then a RG path starting from a non-critical H_0 will pass through all the subspaces of constant ξ with $\xi < \xi_0$. All such trajectories are attracted by one of the two trivial ($\xi^* = 0$) fixed points; either the high temperature fixed point ($H_{T=\infty}^*$) representing total disorder due to vanishing of all couplings, or the low temperature fixed point ($H_{T=0}^*$) for which there is maximum order due to infinite coupling. Although $H_{T=\infty}^*$ is unique, $H_{T=0}^*$ is not necessarily so; e.g. maximum order configurations are different for a ferromagnet and an antiferromagnet.

Of special interest is the $\xi = \infty$ subspace S_∞ , called the critical surface for obvious reasons. S_∞ is an isolated surface separating the two types of trivial fixed points. RG transformation maps S_∞ into itself and the trajectories on

S_∞ are attracted by a non-trivial fixed point H^*_c . H^*_c likewise may not be unique and in that case, S_∞ is divided into domains dominated by each one of the fixed points. The critical behavior of the Hamiltonians within a given domain are imposed by the corresponding H^*_c . However, existence of domains means that there are boundaries which include other relatively unstable fixed points. In fact, $H^*_{T=0}$ and $H^*_{T=\infty}$ are the only stable fixed points and the rest can be classified according to their degree of instability. The instability degree is defined as the number of thermodynamic parameters needed to be fixed for the corresponding criticality condition.

Chapter 4

PHASE TRANSITIONS IN TETRAHEDRAL ISING LATTICE

Critical properties of 3-dimensional systems have been studied with diverse techniques, most notably Monte-Carlo (MC) and RG algorithms. The RG techniques have proved to be not as powerful as in 2-dimensions, however they are faster than MC and give more insight about the physics of whatever is going on. The best estimates of critical exponents in 3-dimensions are obtained by expansion techniques. RG is not quantitatively accurate all the time, but one can usually get a qualitatively correct picture.

4.1 Order-disorder transition in SiGe alloys

In 1985, Ourmazd and Bean [38, 39] reported that they observed for the first time the long-range order in strained SiGe alloy superlattices with alternating double layers of Si and Ge along (111) direction. This bi-layer stacking of Si and Ge can be achieved with two distinct phases. In one of them, the superlattice has the same type of atoms in widely spaced [111] planes (RH1 phase - “AL” in this work), whereas in the second configuration we have closely spaced [111] layers consisting of a single type of atom (RH2 phase - “SL” in this work). Later in 1990, LeGoues *et al.* [40] observed the same order in unstrained superlattices which led to the questioning of the general belief that the order is strain induced. Both SL and AL phases have been experimentally observed. The vanishing of SL phase upon heating and recooling the sample [41] implies the metastability of this ordering related to the growth process [42]. On the other hand, AL phase is found to be reversible [41] putting forward the significance of bulk energetics and thermodynamic properties along with the surface kinetics

in the appearance of the observed phases (see also [43, 44, 45]).

Motivated by these recent experimental findings, a RG study of the SiGe alloy crystal can be performed. Aim is to clarify the relevance of the bulk properties in the occurrence of the observed ordering.

The SiGe superlattice is modelled by a tetrahedrally coordinated Ising lattice where Si atoms are represented by up-spins ($s = +1$) and Ge atoms by down-spins ($s = -1$). The strain due to the lattice mismatch is included into the model by allowing an axial anisotropy in one of the bond directions. This choice is not unique; for example a biaxial anisotropy can be introduced as well. However, the existence of ordering in (111) planes suggests the anisotropy be chosen along one of the four [111] directions. Although the interatomic couplings in the real superlattices are complicated, an approximate picture with nearest (nn) and next-nearest neighbor (nmn) interactions will hopefully preserve the main features of the phase diagram. There exists a strong evidence for the validity of this assumption due to the *ab initio* calculations of couplings in SiGe by Bernard and Zunger [45]. Their calculations yield a nmn -coupling an order of magnitude smaller than nn -coupling term which signals a fast decay of coupling strength with distance.

The next section describes the model and the RG transformation used in the analysis.

4.2 The model and the RG transformation

4.2.1 The model Hamiltonian

We analyze the model defined by the reduced Hamiltonian H ,

$$\begin{aligned}
 H = & K_1 \sum_{\substack{i,j \\ \vec{r}_{ij} = u_a}} s(\vec{r}_i)s(\vec{r}_j) + K_2 \sum_{\substack{i,j \\ \vec{r}_{ij} = u_a}} s(\vec{r}_i)s(\vec{r}_j) \\
 & + J_1 \sum_{\substack{i,j \\ \vec{r}_{ij} = u_a - u_\alpha}} s(\vec{r}_i)s(\vec{r}_j) + J_2 \sum_{\substack{i,j \\ \alpha \neq \beta}} s(\vec{r}_i)s(\vec{r}_j) . \quad (4.1)
 \end{aligned}$$

Here, K_1 , K_2 , J_1 , and J_2 are the interaction constants, obtained by dividing the interatomic pair energies by kT , where k is the Boltzmann constant, and

T is the temperature. s represents the Ising spin variables that can take the values of ± 1 . These spins are located on a tetrahedrally coordinated lattice. We use the notation \hat{u}_a , \hat{u}_b , \hat{u}_c , and \hat{u}_d to represent the four (unit) tetrahedral bond vectors. Since we allow for axial anisotropy in the \hat{u}_a bond direction, we use \hat{u} with a greek index to represent any one of the vectors \hat{u}_b , \hat{u}_c , or \hat{u}_d . The above form for H , then represents a reduced Hamiltonian with nn -interactions (K_1 and K_2), and nnn -interactions (J_1 and J_2). Four-body and higher order interactions are excluded in this analysis.

A physically complete model is expected to include interactions among an odd number of spins, too. These terms will break the up-down symmetry of the Ising model. The relevance of such terms depends on the particular system to be modeled. We will limit our discussion of alloys to systems in which the up-down symmetry is preserved, i.e. those systems in which the alloy is made 50% of one type of atom and 50% of the other, in particular, to the $\text{Si}_{0.5}\text{Ge}_{0.5}$ system. We assume that in such a system, the terms that break the up-down symmetry of the system are cancelled by an appropriate chemical potential contribution to yield a reduced Hamiltonian of the above form.

Construction of blocks

The analysis of the model Hamiltonian in Eqn.4.1 by Kadanoff's block renormalization necessitates the construction of "block spins" out of a number of original spin variables s , in such a way that these new spin variables also form a tetrahedral lattice, with a larger length scale. The recipe for constructing these block spins should be such that if the original spin variables s are ordered in a form corresponding to one of the phases of interest, the block spins should also be similarly ordered. We have chosen a length scale change factor of 3 for our transformation. If a block spin is centered at one of the original spins at point \vec{r} , its four neighbors are located at $\vec{r} - 3\hat{u}_a$, $\vec{r} - 3\hat{u}_b$, $\vec{r} - 3\hat{u}_c$, and $\vec{r} - 3\hat{u}_d$. Then, 27 of the "old" spins s now correspond to a new block spin variable. If the block spin has the same sign as the central original spin when the system is in one of the phases indicated in Table 4.1, then the same kind of order is duplicated in the new system constructed out of the block spins. (Exceptions to this are the phases SL and AL (see Table 4.1) which transform to one another through the transformation. For these phases, the square of the transformation duplicates the type of order.)

In Table 4.2, we list the positions of the original spins (relative to the central position) that form a block spin, and the values of these spins when the system

Table 4.1: Ordered phases of interest

| $s(\vec{0})$ | $s(\hat{u}_a)$ | $s(\hat{u}_b)$ | $s(\hat{u}_c)$ | $s(\hat{u}_d)$ | Name of the phase | Notation |
|--------------|----------------|----------------|----------------|----------------|-------------------------------|-----------------|
| 1 | 1 | 1 | 1 | 1 | Segregated | S |
| 1 | -1 | -1 | -1 | -1 | Zinc Blende | ZB |
| 1 | 1 | -1 | -1 | -1 | Short Si-Ge | AL |
| 1 | -1 | 1 | 1 | 1 | Long Si-Ge | SL |
| 1 | -1 | 1 | -1 | -1 | Short Si-Ge along “b” | AL _b |
| 1 | 1 | -1 | 1 | 1 | Long Si-Ge along “b” | SL _b |
| 1 | 1 | 1 | -1 | -1 | Si-Ge layered in “a-b” planes | AB |
| 1 | -1 | -1 | 1 | 1 | Si-Ge layered in “c-d” planes | CD |

Table 4.2: Spins that form a block

| Relative position of the spin | Number of such spins/cell | Average value of this type of spin in the presence of order | | | |
|---|------------------------------|---|----|---------------|----------------|
| | | S | ZB | AL | SL |
| $\vec{r} = \vec{0}$ (central spin) | 1 | 1 | 1 | 1 | 1 |
| $\vec{r} = \hat{u}_i$ | 4 | 1 | -1 | $\frac{1}{2}$ | $-\frac{1}{2}$ |
| $\vec{r} = 2\hat{u}_i - 2\hat{u}_j, \quad i \neq j$ | 12 | 1 | 1 | 1 | 1 |
| $\vec{r} = 3\hat{u}_i + 2\hat{u}_j, \quad i \neq j$ | 4 | 1 | -1 | $\frac{1}{2}$ | $\frac{1}{2}$ |
| $\vec{r} = 2\hat{u}_i - \hat{u}_j, \quad i \neq j$ | 6 | 1 | -1 | 0 | $-\frac{1}{2}$ |

is perfectly ordered in one of the phases indicated in Table 4.1.

Note that some of these spins are shared by more than one block spin. Note also that some of these spins belong to blocks that are not geographically the closest to them. This enables the inclusion in the block spin of some of the farther away original spins that enhance the ordering of the new system. We determine the sign of the block spin from the majority of the signs of the 13 spins (one at the center of the block, and 12 at a displacement of $2\hat{u}_i - 2\hat{u}_j$, for any pair of bond directions \hat{u}_i and \hat{u}_j). Note that these original spin variables always take the same sign as the center spin for all types of order indicated in Table 4.1. The states of the remaining spins in the block do not contribute to the value of the block spin.

4.2.2 RG transformation

Now, a RG transformation must be constructed such that $H(s) \rightarrow H'(s')$ with the constraint that the Partition function is the same for both Hamiltonians, i.e.

$$Z = \sum_{\{s'\}} \exp(H'\{s'\}) = \sum_{\{s\}} \exp(H\{s\}). \quad (4.2)$$

The next task is to determine H' , i.e. the couplings among $\{s'\}$, using the constraint Eqn.4.2. This can be achieved by assigning values to the new spins s' and evaluating the part of the total partition function through a partial summation over the s variables as dictated by the constraints imposed by the choice of s' . The logarithm of this partial partition function is then a linear function of the renormalized coupling constants, and these new coupling constants can then be determined by solving a set of simultaneous linear equations, each equation being generated by a different choice of configurations of s' . (It is easy to see that this procedure conserves the partition function since a summation of the partial partition functions for all possible configurations of s' releases all constraints on the original spins and hence corresponds to the total partition function.) In general, H' will contain an infinite number of kinds of interactions among the spins. One therefore uses some kind of approximation to determine the renormalized Hamiltonian (see Section 3.2.1). For this purpose, an approximation scheme developed by Kinzel [46] has been adopted to the model defined so far. It enables an approximate determination of H' , while not generating any new types of interactions among the block spins. In this approximation, part of the interactions within the original lattice are treated exactly, while the remaining interactions are decoupled using the mean field approximation

$$\begin{aligned} s_i s_j &= s_i \langle s_j \rangle + \langle s_i \rangle s_j + (s_i - \langle s_i \rangle)(s_j - \langle s_j \rangle) - \langle s_i \rangle \langle s_j \rangle \\ &\approx s_i \langle s_j \rangle + \langle s_i \rangle s_j - \langle s_i \rangle \langle s_j \rangle \end{aligned} \quad (4.3)$$

where $\langle \dots \rangle$ represents the average value of the particular spin while the block spin is constrained to have a certain value dictated by the type of order that is imposed on the new, renormalized system, i.e.

$$\langle s_i \rangle = \frac{\sum_{\{s\}} p(s'; s) s_i \exp H(s)}{\sum_{\{s\}} p(s'; s) \exp H(s)} \quad (4.4)$$

$p(s'; s)$ guarantees that the sums are over the configurations $\{s\}$ which are in agreement with the order imposed on the renormalized system. We have treated the interactions between the central spin of the block and spins connected to it by nearest neighbor interactions exactly, while all other interactions

were decoupled using the mean field approximation, so that the Hamiltonian can be rewritten as

$$H_{ave} = \sum_{i \neq j} K_{ij} s_i s_j + \sum_i \sum_p K_{ip} s_i \langle s_p \rangle + \sum_{p \neq q} K_{pq} \langle s_i \rangle \langle s_j \rangle \quad (4.5)$$

where indices i, j represents any one of the five spins in a block that are treated exactly and p, q represent the spins treated approximately, $\langle s_i \rangle$ is the expectation value of the remaining spins in the block under the imposed order on the block spins, and K_{ij} is one of K_1, K_2, J_1, J_2 or zero depending on the distance r_{ij} . Replacing H by H_{ave} in Eqn.4.4, we get an implicit equation for all $\langle s_i \rangle$ (since H_{ave} includes them) which must be solved self consistently. In general, the expectations $\langle s_i \rangle$ are different for all spins, therefore the number of unknowns are too many to be solvable for an arbitrary configuration $\{s'_i\}$. However, restricting the renormalized Hamiltonian to have the same type of interactions, Eqn.4.5 can be solved by considering several symmetric configurations. In our case, this involves the self consistent evaluation of 41 spin averages, under the 8 different constraints imposed by the types of order indicated in Table 4.1.

The partial sums in Eqn.4.4 can be evaluated in terms of unrestricted sums using the following mathematical trick :

For simplicity, assume that $s_i = 0, 1$ and let S' be a partial sum to be evaluated :

$$S' = \sum_{\{s\}} p(s'; s) f(s_1, \dots, s_N). \quad (4.6)$$

The restriction $p(s'; s)$ on the sum is that $\sum_i s_i > N/2$. This is the majority law over the 13 spins defined previously. Define a function of complex variable z as :

$$S(z) = \sum_{\{s\}} z^{(s_1 + \dots + s_N)} f(s_1, \dots, s_N) \quad (4.7)$$

so that $S(1)$ is the unrestricted sum over all spins. For $N < \infty$, above sum can be expanded as a finite power series in z :

$$S(z) = a_0 z^0 + a_1 z^1 + \dots + a_N z^N. \quad (4.8)$$

Then, the original sum in 4.6 is expressed in terms of a_k as

$$S' = a_j + \dots + a_N, \quad N/2 < j < N/2 + 1. \quad (4.9)$$

$S(z)$ becomes a Fourier sum for $z = e^{i2\pi/(N+1)l}$:

$$S'(e^{i\frac{2\pi}{N+1}l}) = \sum_{k=0}^N a_k e^{i\frac{2\pi}{N+1}kl}. \quad (4.10)$$

Each Fourier coefficient a_k can be calculated using the inverse Fourier transform

$$a_j = \frac{1}{N+1} \sum_{l=0}^N e^{-i\frac{2\pi}{N+1}jl} S(e^{i\frac{2\pi}{N+1}l}). \quad (4.11)$$

The transformation involves solving a set of linear equations involving coupling constants K_1, K_2, J_1, J_2 and a fifth parameter, a constant term in the Hamiltonian conserving the total free energy of the system. Each type of ordering of spins gives a linear equation in transformed couplings through the relations expressed in Eqn.4.2 and Eqn.4.4. However, since the number of RG parameters to be solved is five, the four types of order considered so far are not enough to realize the transformation. Therefore, average magnetizations are calculated for four more types of ordering which are listed in Table 4.1. The necessity of considering four more configurations to get eight linearly independent equations of five unknowns is due to symmetry constraints, i.e. the transformed couplings should exhibit the same symmetries as the original Hamiltonian.

Finally, we have a system of equations which can be written in matrix form as

$$Ax = b. \quad (4.12)$$

Eqn.4.12 does not have a solution for the resulting A . Instead, we find an approximate solution for x giving the least square error, which after some linear algebra can be written down as

$$x_{ls\epsilon} = (A^T A)^{-1} A^T b. \quad (4.13)$$

This final step completes the transformation. In the next section, the outcomes of the transformation will be presented.

4.3 Results and the Phase Diagram

The accuracy of the transformation can be checked by comparing with the previous exact or well-established results. Two special cases for which the problem reduces to two dimensions will be considered for this purpose. First, letting $K_1 = J_1 = J_2 = 0$, we have a triangular lattice in each [111] plane decoupled from the rest of the volume, because the interlayer couplings indexed by '1' are zero. Second, letting $K_1 = K_2 = J_1 = 0$, we get a honeycomb lattice which again is isolated in [111] planes. Both cases are expected to give $2D$ critical exponents. Note that one may obtain a quasi- $2D$ system by choosing

Table 4.3: Comparison of results of this work with established results

| Special case | Critical value | | Critical exponent (ν) | |
|--|----------------|--------------|-----------------------------|------------|
| | this work | other work | this work | other work |
| 2D Ising model on a honeycomb lattice ($K_1 = J_1 = J_2 = 0$) | .412 | .6585 * [47] | .820 | 1* |
| 2D Ising model on a triangular lattice ($K_1 = K_2 = J_1 = 0$) | .1908 | .2746 * [47] | .910 | 1* |
| 3D Ising model on a tetrahedral lattice ($K_1 = K_2, J_1 = J_2 = 0$) | .2930 | | .780 | .632 |

* exact result

$K_2 = J_1 = 0$. However, it is well-known that such planar systems with finite thickness exhibit the same type of critical behavior as $2D$ systems, i.e. share the same critical exponents. Isotropic tetrahedral lattice with nm -coupling only is also treated as a special case in three dimensions for which no previous work in the literature exists.

For all of these cases, the critical couplings, i.e. Hamiltonian flowing to the nontrivial fixed point of the transformation is found and the corresponding critical exponent ν is calculated by linearizing the transformation around the fixed point as described in Section 3.3. Note that the first system in Table 4.3 does not represent a fixed point since a nonzero K_2 induces a nonzero J_2 in the succeeding iterations. It is nevertheless a critical point which at each iteration approaches to a fixed point with $K_1 = J_1 = 0$. On the other hand, the second special case is a highly unstable fixed point in the sense that if one of the vanishing couplings is turned on slightly, the Hamiltonian flows to another (“crosses over” in RG terminology), more stable fixed point. Table 4.3 lists the critical parameters obtained by the described RG transformation together with previous works in the literature. It should be noted here that the choice of the particular spins that construct the block spins is not optimal for some of the special cases shown in the table. The value of ν for three dimensions is almost the same as the value found by Kinzel [46] in his application of this RG method to a $3D$ cubic lattice.

It is useful to note here that this RG transformation is not designed to handle the special case of the frustrated phase that is expected to occur when the next nearest neighbor coupling is sufficiently negative. A better transformation

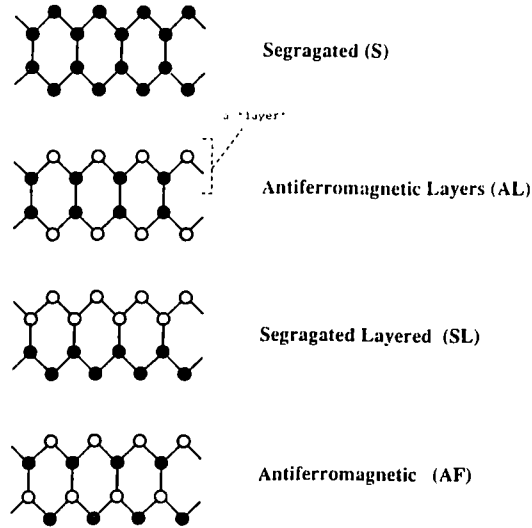


Figure 4.1: Relative positions of atoms for the types of orders corresponding to each fixed point. Filled and empty sites represent opposite spins.

would involve the expansion of the degrees of freedom to include the possibility of defects, as for example in the transformations used by Berker, et al. [48]. The chaotic renormalization group trajectories that are characteristic of such phases are not observed (for an example see [49]). The trajectories here that correspond to this phase however, do indeed have some peculiar characteristics which is explained in the next section.

4.3.1 The Phase Diagram

With the restricted form of the Hamiltonian as presented in Equ.4.1, the only ordered phases that will appear are the S, AF, SL, and AL phases. Fig.4.1 shows the corresponding ordering of atoms in $[110]$ planes. Note that the phases AL and SL contain layers of identical atoms perpendicular to (111) direction, whereas AF is the completely antiferromagnetic tetrahedral lattice. The phase diagram will be presented only for a restricted set of these phases, because the symmetry in the Hamiltonian allows one to go from one ordered phase to another by changing the signs of some of these interactions. As a result of this symmetry, for example the critical fixed points belonging to each one of the orderings in Fig.4.1 can be deduced from a single one of them, e.g. the fixed point of the S phase, using the symmetries of the Hamiltonian listed in Table 4.4. In other words, these four fixed points differ only by the *signs* of the couplings.

Table 4.4: Symmetries of the Hamiltonian

| Original phase | K_1 | K_2 | J_1 | J_2 | New phase |
|----------------|--------|--------|--------|-------|-----------|
| S | $-K_1$ | K_2 | $-J_1$ | J_2 | SL |
| S | $-K_1$ | $-K_2$ | J_1 | J_2 | AF |
| S | K_1 | $-K_2$ | $-J_1$ | J_2 | AL |

However, the Hamiltonian (and therefore the phase diagram) is not symmetric with respect to all sign changes: When next nearest neighbor interactions are negative and dominant, the spins will prefer a frustrated state to minimize the total energy. This can be demonstrated by a straightforward Monte Carlo simulation. Being more specific, frustration may occur when $J_2 < 0$ or when $J_1 < K_1 \cdot K_2$ for which the interactions have a competitive nature. Although this domain is not of major interest to us, and it is questionable whether the presented renormalization group transformation is sufficiently equipped to handle this special phase, one does see the effects of this phase in the renormalization group trajectories. As an example, Fig.4.2 shows the phase boundaries as well as the renormalized couplings after a single iteration of the RG transformation along the phase boundary for the isotropic Hamiltonian. All points on the phase boundary eventually renormalize to a fixed point. However, only the points on the bold portion of the plot approach the fixed point in a regular fashion, i.e. points closer to the fixed point map into even closer points. On other parts of the boundary, the transformation results in a rather abrupt jump onto this regular critical domain, some points transforming to the fixed point directly, in a single iteration. As can be seen from Fig.4.2, all phase boundary points to the left of point P (which corresponds to the maximum of the K' vs. J curve) show this unusual type of RG flow characteristics, an apparent effect of the frustrated phase that is expected to occur in this domain. Although one could classify all points that generate this type of unusual RG trajectories as belonging to the frustrated phase, due to the uncertain amount of accuracy of such a classification, this region of the phase space will be excluded from the analysis.

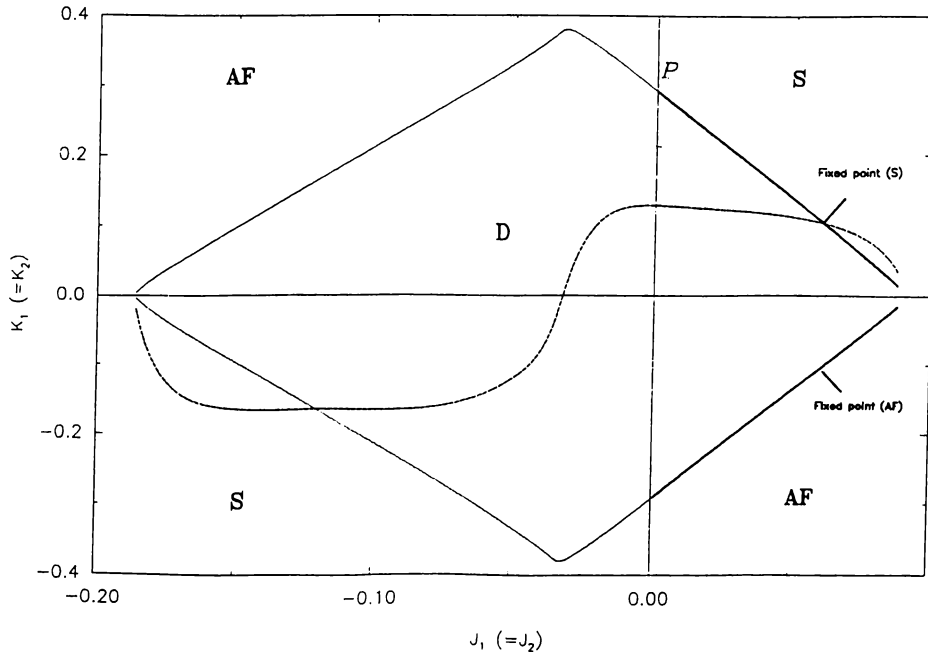


Figure 4.2: Phase diagram for the isotropic tetrahedral Ising lattice. The bold portion of the phase boundary indicates the region where the RG transformation is expected to be reliable. Dashed curve is a plot of K' (of the transformed Hamiltonian) vs J (of the original Hamiltonian) generated after a single RG transformation applied to the points with $K > 0$ on the given phase boundary. The flow towards the fixed point is regular *only* for the bold region (left of P) where J is positive. For details refer to the text.

Since $J_2 < 0$ is sufficient to induce frustration and $J_2 < 0 < J_1$ can be mapped to another system with $J_1, J_2 > 0$, it is suitable to investigate the phase space for J_1 and J_2 both positive. Furthermore, the anisotropy will be introduced through the mn -interactions, keeping $J_1 = J_2$. This is a good assumption if mn -couplings are an order of magnitude (or more) stronger than mnn -couplings which is verified by *ab initio* calculations [45]. Note that the RG transformation will still generate unequal values of J_1 and J_2 in the successive iterations. The phase diagrams are obtained by following the RG trajectories for the corresponding initial coupling constants until one gets sufficiently close to a particular high or low temperature fixed point.

Fig.4.3 shows the critical surface and the fixed point on it corresponding to the S phase. The base plane corresponds to $T = 0$ and the phase boundaries which are exact are shown with dashed curves. All points above the critical surface flow to the high temperature fixed point whereas the points below the critical surface are in the domain of the corresponding ordered phase. The bottom of the valleys on the critical surface correspond to the critical end-points of first-order transition lines. Each slope of a valley belongs to the

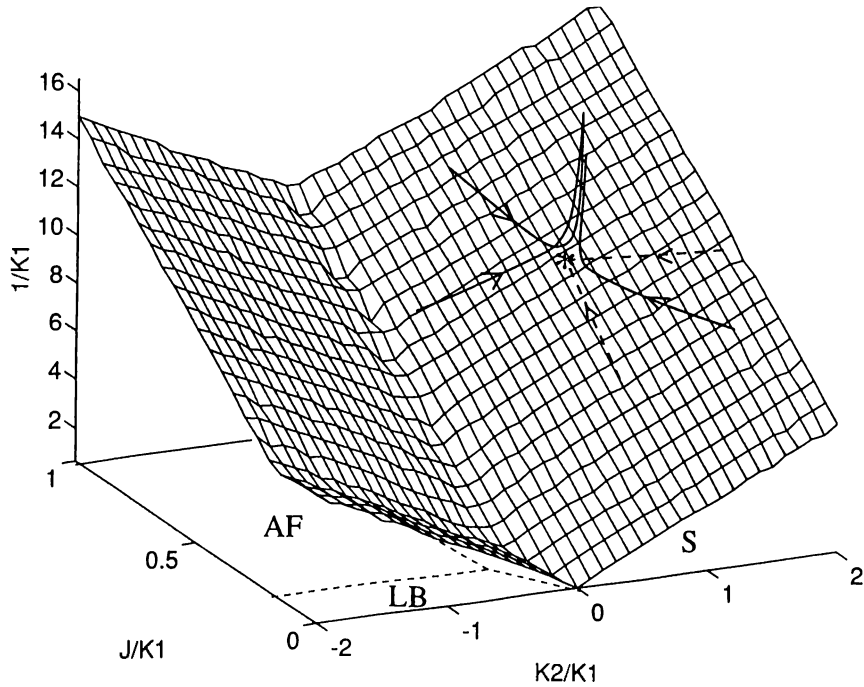


Figure 4.3: The critical surface for the anisotropic tetrahedral Ising lattice with $J_1 = J_2 > 0$ as a result of the RG analysis. The fixed point of the S phase is indicated and several RG flows above (solid) and on (dashed) the critical surface are shown schematically.

domain of a different critical fixed point. The topology of the critical surface is illustrated in Fig.4.4. The critical fixed points representing each one of the orderings shown in Fig.4.1 are separated by domain walls on which lay relatively unstable fixed Hamiltonians with some of the interactions in Eqn.4.1 missing. In between them lay still more unstable fixed points, with more couplings to be fixed. The Hamiltonian for the 2-dimensional triangular lattice listed in Table 4.3 is one of these.

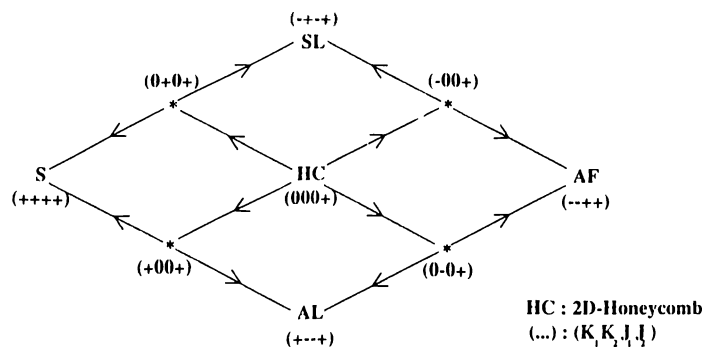


Figure 4.4: The topology of the critical surface. On the corners are the four most stable fixed points corresponding to each ordering. In between are the more unstable fixed points (some of them are skipped to avoid complexity).

The actual two-body interactions for the bulk SiGe have been estimated previously by Bernard and Zunger through *ab initio* calculations [45]. Their results predict $K = -2.48\text{meV}$ and $J = 0.15\text{meV}$. These couplings, when inserted into the phase diagram predict a very low transitions temperature which supports the belief that the observed long-range order is induced by surface effects rather than the bulk properties.

Chapter 5

CONCLUSION

Using RG approach, the phase diagram for the tetrahedral Ising lattice is obtained with anisotropic nearest neighbor and next nearest neighbor interactions. With the allowed anisotropy to break the symmetry along a tetrahedral bond direction, one can obtain four different ordered phases. Fixed points corresponding to the phases are related to each other by transformations involving sign changes of the couplings. The critical exponents for $3D$ and $2D$ are calculated by linearizing the transformation around the fixed points. Results are in agreement with the values obtained for systems in the same universality classes.

Considering the SiGe crystal in this context and using values of couplings obtained through the crystal energies for different configurations (see [44]), one obtains relatively low transition temperatures due to the small energy differences between the different phases. Furthermore, the critical fixed points for each one of the phases differ only by the signs of some of the couplings, so that the isotropic fixed point remains stable in this new scheme with an extended set of parameters. Therefore, it can be concluded that a slight anisotropy in the bulk interactions is not sufficient for appearance of a new ordering (SL or AL) in SiGe. Our results indicate (in agreement with the previous work [44]) that surface-kinetic effects rather than the bulk thermodynamic effects dominate the observed ordering during the growth of SiGe alloys.

Apart from the primary motivation concerning SiGe alloys, the present study can be used as a starting point for any RG application on tetrahedrally coordinated systems. Although the present structure of the model is not suitable for handling spin-glass phases properly, it may be developed further by allowing for more than two spin states which hopefully will create the expected chaotic trajectories for the frustrated phases.

References

- [1] Weast R.C. *Handbook of Chemistry and Physics* (CRC Press, Boca Raton, Florida), 1981, p. F-76.
- [2] Andrews Th., *Phil. Trans. R. Soc.* **159**, 1869, p. 575.
- [3] Van der Waals J.D. Thesis D, 1873.
- [4] Klein M.D., *Physica* **73**, 1974, p. 28.
- [5] de Boer J., *Physica* **73**, 1974, p. 1.
- [6] Levelt-Sengers J.M.H., *Physica* **73**, 1974, p. 73.
- [7] Weiss P., *J. Phys.* **6**, 1907, p. 661.
- [8] Landau L.D., *Phys. Z. Sowjetunion* **11**, 1937, 545.
- [9] Van der Waals J.D., *Verh. Kon. Akad. Wetensch. Amsterdam* **14 II**, 1983, nr. 8 ; *Z. Physik. Chemie* **13**, 1984, p. 657.
- [10] Van Laar J.J., *Proc. Kon. Akad. Sci. Amsterdam* **14 II**, 1912, p. 1091.
- [11] Verschaffelt J., *Comm. Leiden* **18**, 1895.
- [12] Verschaffelt J., *Comm. Leiden* **28**, 1896.
- [13] Verschaffelt J., *Comm. Leiden* **55**, 1900.
- [14] Stanley H.E., *Introduction to Phase Transitions and Critical Phenomena*, Oxford Science Publications (Oxford University Press, New York), p. 10.
- [15] Goldhammer D.A., *Z. f. Physik. Chemie* **71**, 1910, p. 577.
- [16] Van der Waals J.D., *Verhandelingen, Kon. Akad. Wet. Amsterdam* **20**, 1880.
- [17] Kamerlingh Onnes H., *Verh. Kon. Akad. Wetensch. Amsterdam* **21**, 1881; *Comm. Leiden* **23**, 1886.

- [18] Fisher M.E., *J. Math. Phys.* **5**, 1964, p. 944.
- [19] Essam J.W., Fisher M.E., *J. Chem. Phys.* **38**, 1963, p. 802.
- [20] Widom B., *J. Chem. Phys.* **41**, 1964, p. 176.
- [21] Widom B., *J. Chem. Phys.* **43**, 1965, p. 3892.
- [22] Wilson K.G., Kogut J., *Phys. Rep.* **12C**, 1974, p. 75.
- [23] Wilson K.G., *Rev. Mod. Phys.* **47**, 1975, p. 773.
- [24] Stanley H.E., *Phys. Rev.* **176**, 1968, p. 718.
- [25] Kadanoff L.P., *Physics* **2**, 1966, p. 263.
- [26] Niemeijer Th., van Leeuwen J.M.J., *Phys. Rev. Lett.* **31**, 19973, p. 1411.
- [27] van Leeuwen J.M.J., *Phys. Rev. Lett.* **34**, 1975, p. 1056.
- [28] Nauenberg M., Nienhuis B., *Phys. Rev. Lett.* **33**, 1975, p. 944.
- [29] Onsager L., *Phys. Rev.*, **65**, 1944, p. 117.
- [30] Swendsen R.H., *Phys. Rev. Lett.*, **42**, 1979, p. 859.
- [31] Binder K., *Monte Carlo Methods in Statistical Mechanics*, Topics in Current Physics, Vol.7 (Springer, Berlin, Heidelberg, New York), 1979.
- [32] Brukhardt T.W., van Leeuwen J.M.J., *Real-Space Renormalization*, Vol.30 (Springer-Verlag, Berlin, Heidelberg, New York), 1982.
- [33] Hilhorst H.J., Schick M., van Leeuwen J.M.J., *Phys. Rev. Lett.* **40**, 1978, p. 1605.
- [34] Kadanoff L.P., Houghton A., *Phys. Rev. B* **11**, 1975, p. 377.
- [35] Kadanoff L.P., *Phys. Rev. Lett.* **34**, 1975, p. 1005.
- [36] Kadanoff L.P., Houghton A., Yalabik M.C., *J. Stat. Phys.* **14**, 1976, p. 171.
- [37] Widom B., *J. Chem. Phys.* **43**, 1965, p. 3898.
- [38] Ourmazd A. Bean J.C., *Phys. Rev. Lett.* **55**, 1985, p. 765.
- [39] Lockwood D.J., Rajan K., Fenton E.W., Baribeau J.-M. and Denhoff M.W., *Solid State Comm.*, **61**, 1987, p. 465.
- [40] LeGoues, F.K., Kesau, V.P., Iyer, S.S., *Phys. Rev. Lett.*, **64**, 1990, p. 40.

- [41] Muller E., Nissen H.-U., Mäder K.A., Ospelt M. and von Känel H., *Phil. Mag. Lett.*, **64**, 1991, p. 183.
- [42] LeGoues, F.K., Kesan, V.P., Iyer, S.S., Tersoff J. and Tromp R., *Phys. Rev. Lett.*, **64**, 1990, p. 38.
- [43] Ciraci S., Baratoff A. and Batra I.P., *Phys. Rev.*, **B 41**, 1990, p. 6069.
- [44] de Gironcoli S., Giannozzi P. and Baroni S., *Phys. Rev. Lett.*, **66**, 1991, p. 2116.
- [45] Bernard J.E., Zunger A., *Phys. Rev. B*, **44**, 1991, p. 1663.
- [46] Kinzel W., *Phys. Rev. B*, **19**, 1979, p. 4584.
- [47] Baxter R.J., *Exactly Solved Models in Statistical Mechanics* (London: Academic Press), 1984.
- [48] Berker N., Ostlund S. and Puntam F.A., *Phys. Rev. B* **17**, 1978, p. 3650.
- [49] McKay S.R., Berker A.N. and Kirkpatrick S., *Phys. Rev. Lett.* **48**, 1982, p. 767.